THE EVOLUTION OF THE EAST ASIAN ENVIRONMENT

VOLUME I
Geology and Palaeoclimatology

Editor
ROBERT ORR WHYTE

THE COINCIDENCE OF A GENERAL CLIMATIC MODEL AND HISTORICAL CLIMATIC OBSERVATIONS IN EAST ASIA

Bruce Denness

[*Offprint*]

Centre of Asian Studies
UNIVERSITY OF HONG KONG
1984

THE COINCIDENCE OF A GENERAL CLIMATIC MODEL AND HISTORICAL CLIMATIC OBSERVATIONS IN EAST ASIA

Bruce Denness

Introduction

Geologists have for many years recognised the variability of palaeo-climates from the geological record. Over hundreds of millions of years the Earth has passed into and out of ice ages and desert conditions leaving tell-tale evidence in sedimentary rocks. Until recently, however, this multitude of climate-related data remained largely uncorrelated. Then Denness (in press) illustrates that it is possible to derive a single analytical expression that will accommodate a description of reliable proxy climatic time series data over any range of timescales before 1,000,000 years B.P. The expression, which describes global temperature and related climatic data, is in the form of sine series and may be given as:

$$G(t) = \sum_{n = N(T)}^{\infty} A(T)a^{n}.\ \sin b^{n-1}\pi\left(\frac{t}{T}\right)$$

zero registered at time T_o

Where G(t) is a time based climatic index,

A(T) is the amplitude of a reference periodicity T,

N(T) is the reference integer for periodicity T,

a,b are absolute constants, here taken as 0.84 and 2.0 respectively,

n is an integer, i.e. the reference number of a particular sine component,

and t is time in years

Denness (1981) had already suggested that the expression could also be used to describe time series matching observed climate-related data over the more recent timescales of the Quaternary period, even within the historical record. To substantiate that, this paper will demonstrate the mathematical model's ability to match (hindcast) measured time series over a range of timescales up to 1,000,000 years B.P., thereby extending its capacity throughout the geological and historical timescales. This enables confidence to grow in the likelihood that the model may be used in predictive mode. As an illustration of this possibility the model is then extended into higher frequencies (not tested in this paper) and is found to match several climatic time series over the most recent few hundred years in China and Japan.

The comparison of model and observed records is done here graphically by superimposing selected time series data on to computer-drawn, moving average plots from the "fundamental" equation. In so doing we are seeing the variaton of the sum of a series of sine curves, each successively smaller component being of 0.84 times the amplitude of its more fundamental neighbour and of half the period. The extension of the model into the historical period adds a further 11 sine components to the 13 already illustrated for the Phanerozoic and beyond by Denness (in press).

As in the earlier work the following figures have resulted from the application of a moving average technique to series of values of G(t) before plotting the derived $G_{ma}(t)$ to remove the higher frequencies from each plot. This was done in an attempt to secure compatibility of sensitivity between the climate model and the measured data. To achieve this the time interval for each diagram was divided into 600 portions for each of which G(t) was calculated and then subjected to a moving average analysis over successive groups of 100 points resulting in the following plots which consequently use 500 data points each. In order that each moving-average plot should commence at the present time (zero, B.P.) it was necessary to use the predictive quality of the equation to foresee 50 data points into the future for each timescale. Consequently the degree of success in matching the latest (nearest zero B.P.) 10 per cent of the plots to the observed data could be seen as a preliminary assessment of these predictive capabilities.

The technique generally used to overlay the observed time series data, all of which have been culled from the literature, was to photograph the figure and place the negative in an enlarger so that its image could be superimposed at the appropriate timescale on to the $G_{ma}(t)$ graph which had been previously prepared by x-y plotter. Apart from errors involved in tracing the image by hand this preserves the accuracy of the measured data and renders it readily recognisable from the original source. The

advantage of preserved integrity is offset to some degree by the consequent inconsistencies of ordinate scale. However, no serious attempt is intended here to derive absolute temperature (or other) amplitudes but merely to demonstrate the consistent compilation of a regular sine series with ordered periodicities. In addition some data required processing to be compatible with the common presentation; this is noted where appropriate.

The reader is referred to the original publications for additional information concerning the reasons to suppose that the variables are climatically related. Equally the original publications are the best sources of reference to dating accuracy, which the writer here notes to be somewhat irregular between the various records. All the figures use essentially local data but from many different sites throughout the world.

Testing the model

In the following section six different timescales are examined, each beginning at the present day but ranging from the first time series of up to 1,000,000 years B.P. through successively shorter periods down to 1,800 years B.P.

0-1,000,000 years B.P.

Figure 1 is a slightly reduced version of Figure 5 from Denness (in press) and serves to provide continuity with the earlier work. While the major component evident here may be considered as fundamental to the present thesis it is thus seen as but a small harmonic of an earlier "fundamental" period of climatic variation. Figure 1 depicts the progress of two separate records of oxygen isotope ratio from the Challenger Plateau as reported by Shackleton and Kennett (1975) and the tropical Atlantic by Van Donk, from 1,000,000 years to the present superimposed on the G_{ma} (t) plot. The more sensitive isotope ratio plot and that for ice volume clearly indicated a primary maximum (arrowed) corresponding approximately to that of the G_{ma} (t) plot at about 0.4×10^6 years with neighbouring minima (arrowed) offset in the saw-toothed pattern typical of the G_{ma} (t) plot at all timescales. This draws attention to support for a variation with period about 549,200 years as does the less sensitive isotope ratio curve which also clearly indicates a further maximum (arrowed) at about 950,000 years.

0-170,000 years B.P.

The literature has not made available to the writer clear evidence of the anticipated 274,600 year periodicity, though readers may notice the ghost of such a feature in the records given in Figure 1. However, Figure 2 restores the series with the general trend of each of the

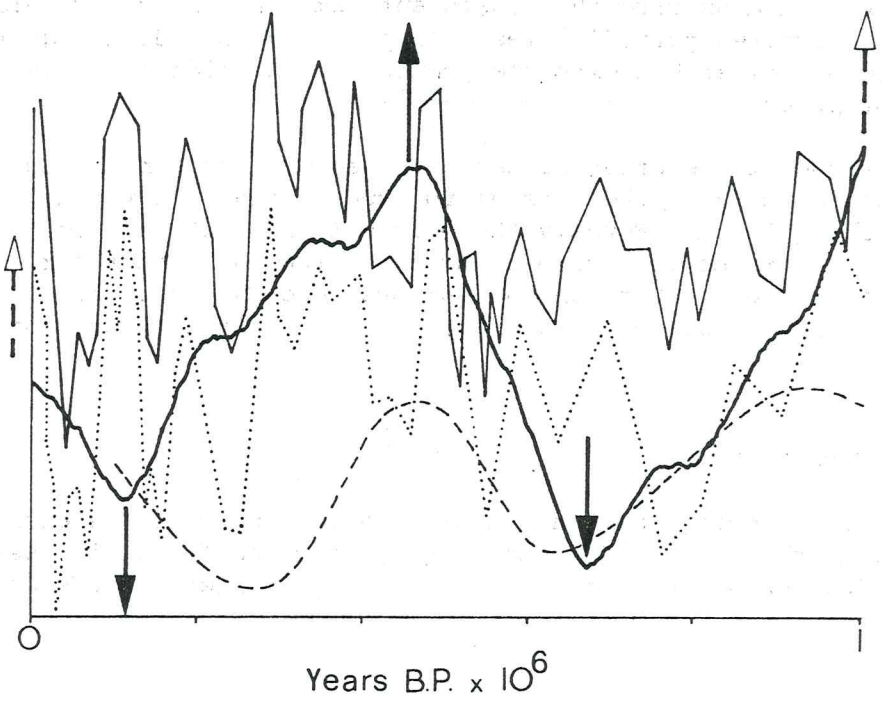

a) Model

b) Oxygen isotope ratio for tropical Atlantic

c) Oxygen isotope ratio for Challenger Plateau

d) Volume of glacial ice.

Note the coincidence of maxima and minima of the observed time series with those of the model (arrowed)

Figure 1 Comparison of climatic indices and model on the timescale 0-1,000,000 years B.P.

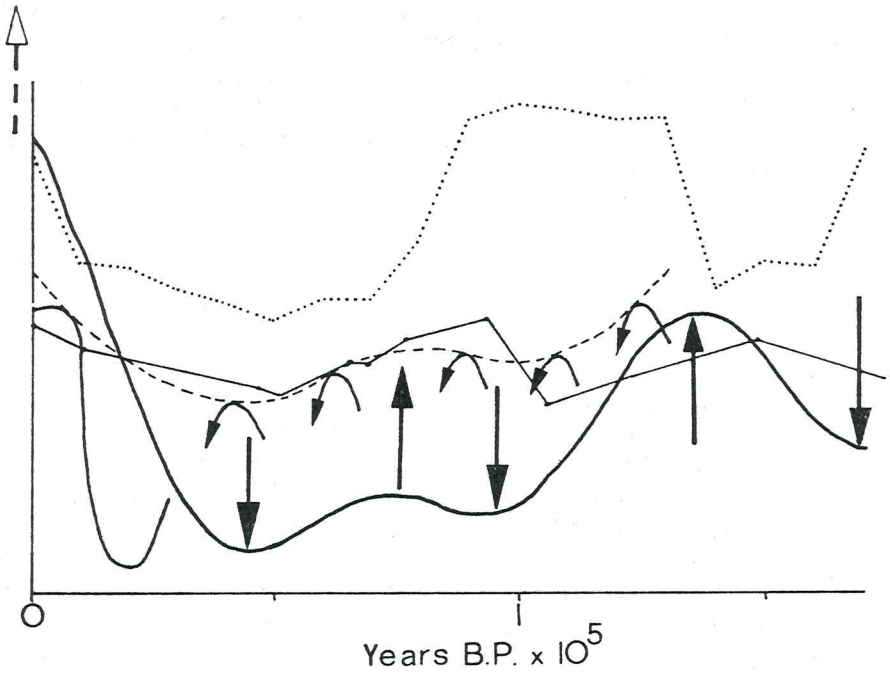

Figure 2 Comparison of climatic indices and model on the timescale 0-170,000 years B.P.

observed records responding to the 137,300 years periodicity emphasized by the maxima indicated by the hollow arrow to the left of the diagram and the upward arrow most towards the right with the interposed minimum at the site of the most leftward downward arrow on the $G_{ma}(t)$ curve. The three types of data are an isotopic temperature curve from the Caribbean reduced from a more detailed plot by West (1972), a generalized sea level curve obviated here from original data of Bloom (1971), and a carbonate curve from the equatorial Pacific prepared by Hays *et al.* (1969). Each of the observed data series also draws attention to the next periodicity in the series at 68,650 years emphasized by considering all the upright arrows.

0-100,000 years B.P.

The 68,650 year periodicity becomes the general trend of all the observed data in Figure 3. This diagram again presents three data series for correlation with the $G_{ma}(t)$ plot. Here they are the oxygen isotope ratio from a Greenland ice core analysed by Dansgaard *et al.* (1971), July temperatures from insect analysis in the Netherlands by Van der Hammen *et al.* (1967), and the abundance of Mediterranean tree pollen described by Van der Hammen *et al.* (1971). In addition the majority of each of the observed records exhibits general maxima and minima at each of the major arrows on the $G_{ma}(t)$ plot, illustrating a further periodicity of about 34,330 years. Though it is not necessary to extract more detail from this figure, the Greenland isotope ratio curve in particular could also be called in evidence of the next higher frequency in the series at 17,170 years.

0-25,000 years B.P.

Proceeding to Figure 4 three more climate-related records are compared with the $G_{ma}(t)$ plot; these are the February sea surface temperature in the tropical Atlantic as determined from foram species populations by Imbrie and Kipp (1971), averaging temperature in Colombia, South America deduced from vegetation changes by Heussen (1966), and the generalized temperature for the middle latitudes of the northern hemisphere prepared from treeline studies by La Marche (1974). The general trend of these records, particularly the tropical Atlantic and northern hemisphere data, emphasises the 17,170 years period. In turn, all the major arrows in concert draw attention to the next component in the series of periodicities at 8,580 years.

0-6,000 years B.P.

Figure 5 describes the variation of three more climate-related variables for comparison with $G_{ma}(t)$ plot. Here is seen the variation of *Eucalyptus* pollen abundance at Boggy Lake in southwestern Australia deter-

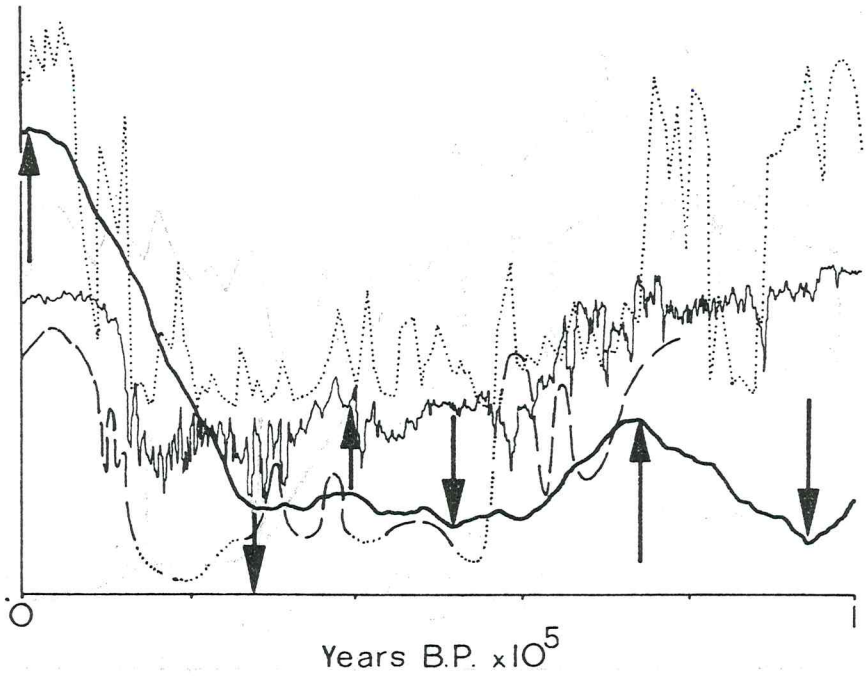

Figure 3 Comparison of climatic indices and model on the timescale 0-100,000 years B.P.

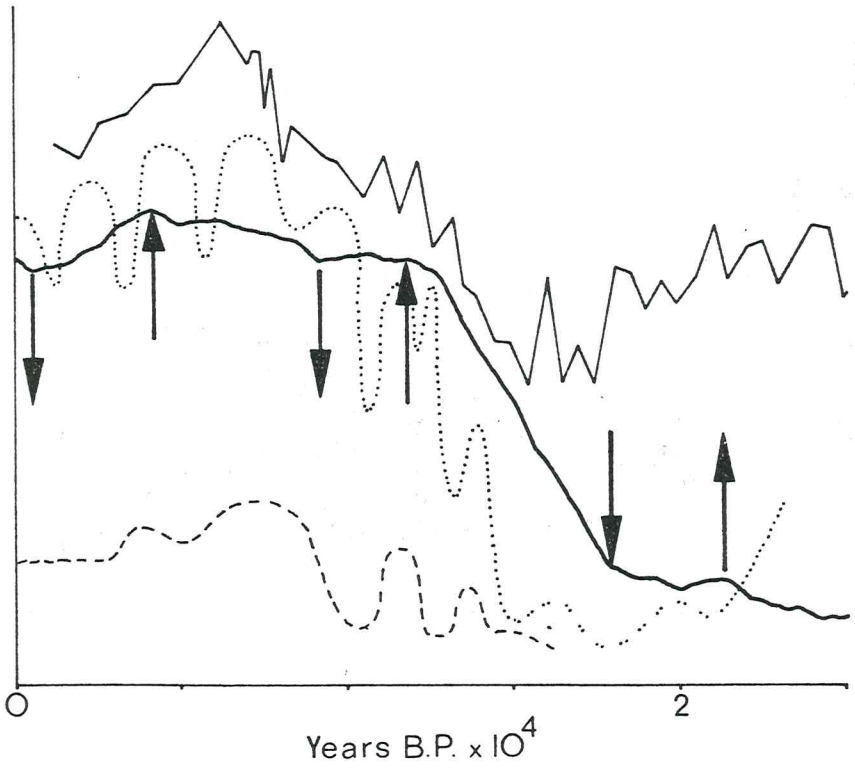

a) Model

b) February sea surface temperature in the tropical Atlantic

c) Annual temperature in Colombia, S. America.

d) Generalized temperature for middle latitude of northern hemisphere

Note the coincidence of maxima and minima of the observed time series with those of the model (arrowed)

Figure 4 Comparison of climatic indices and model on the timescale 0-25,000 years B.P.

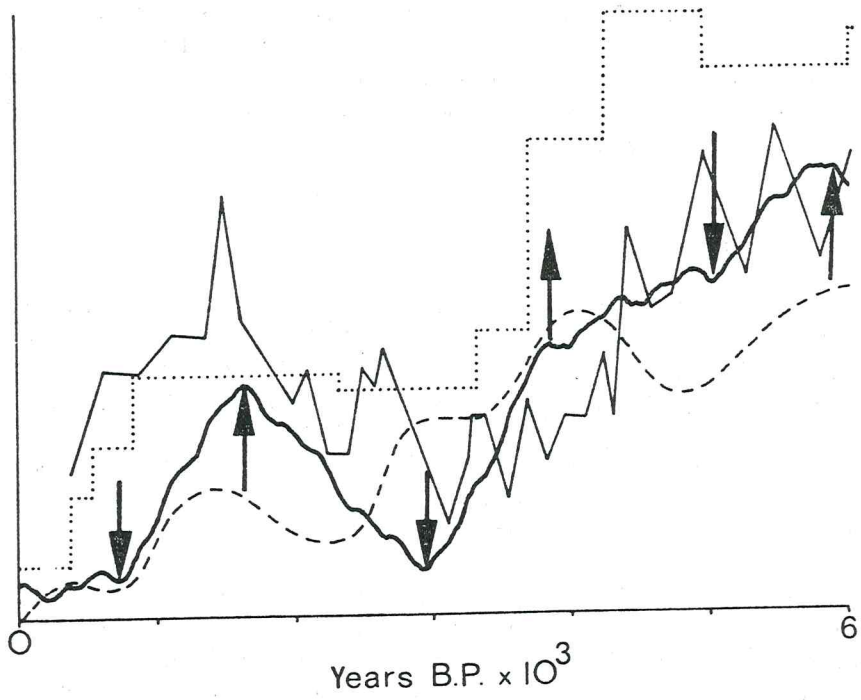

a) Model

b) Eucalyptus pollen abundance in southwestern Australia

c) Altitude of upper treeline in the Alps.

d) Altitude of upper treeline in California

Note the coincidence of maxima and minima of the observed time series with those of the model (arrowed)

Figure 5 Comparison of climatic indices and model on the timescale 0-6,000 years B.P.

mined by Churchill (1968), the generalized changing altitude of the upper treeline in the Alps and other temperate mountain regions evaluated by Markgraf (1974), and the varying altitude of the upper treeline on one specific mountain, Sheep Mountain, in California reported by La Marche (1973). The general trend, peaking at 1600 and almost 5900 years B.P. with the major trough at about 3000 years B.P. outlines the next anticipated periodicity of 4,290 years; this is particularly reflected by the California treeline and Australian pollen abundance variations. The next expected component of periodicity 2,180 years is only weakly represented in the observed data but nevertheless coincidence with this period in the $G_{ma}(t)$ curve is noted for most of both the treeline plots and the latter part of the pollen variation.

0-1,800 years B.P.

The variation of three more climate-related records is described along with the $G_{ma}(t)$ plot in Figure 6. Essentially the same trends are noted for the deuterium proportion in bristlecone pines of California described by Lamb (1977) and based on data from Dr. Irving Friedman, global glacier advances researched by Bray (1968) and the drift of the winter severity index across Europe at 50°N determined by Lamb (1977). The major arrows draw attention to a periodicity of about 1,090 years in the variation of the $G_{ma}(t)$ plot which is reflected in the general behaviour of each of the recorded data series. It is also suggested that judicious correlation of the maxima and minima represented by the minor arrows on the $G_{ma}(t)$ curve with general peaks and troughs on certain of the recorded data plots lend credence to the existence of higher frequency variations, though this does not constitute part of the current thesis.

Extrapolation of the model to east Asia

Having developed the climate model and tested it over geological and prehistoric time scales through this paper and the early work by Denness (in press), let us now turn to its application in East Asia. At the same time, let us consider the possibility of extending the sine series from its tested minimum periodicity of 1,090 years through the lower anticipated periods of climatic variation of 545, 272 and 136 years respectively. This represents not only a regional calibration of the equation but also the demonstration that higher frequencies than those already tested can be successfully predicted.

China

Figure 7 is a rather complicated diagram portraying the variation of the three Chinese climatic variables, raininess, temperature and cloudiness, along with the $G_{ma}(t)$ plot over the most recent 600 years of history. The major upward arrows at each end of the $G_{ma}(t)$ plot (solid to the left

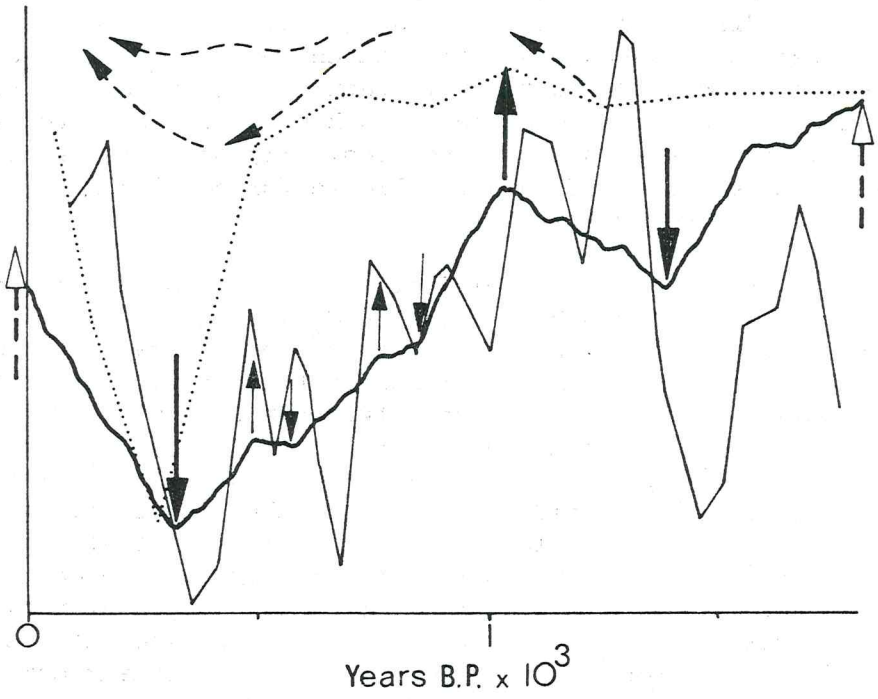

Figure 6 Comparison of climatic indices and model on the timescale 0-1,800 years B.P.

and hollow to the right) represent maxima of the 545 year period of the $G_{ma}(t)$ curve for which there is no corresponding record of variation of the climatic variables over this relatively short timespan. However, both the 272 and 136 year periods are represented in all the records.

Let us first compare the variability of the Chinese climatic records with each other. The vertical dotted lines accentuate the logical direct link between cloudiness as determined by Link (1958) and raininess represented by the "raininess" index of Yao (1943, 1944) described by Schove (1949). The vertical dashed lines draw attention to the inverse link between these two properties and the temperature as given by Chu Ko-chen (1973). While the latter inverse relationship (i.e. the hotter the temperature the wetter the climate) is not logically predictable, it is consistent with the behaviour of Chinese climate forthcoming from global modelling performed by Wigley *et al.* (1980).

With the above relations in mind it is now appropriate to examine the correlation of climatic variables with the $G_{ma}(t)$ plot. Allowing for the minor adjustment in the timing of the maxima and minima of the measured climatic data emphasized by the small horizontal arrows, a reasonable degree of consistency is demonstrated between these times and those of the corresponding maxima and minima pointed out by major arrows on the $G_{ma}(t)$ curve. Because of the interdependence of all three climatic variables it is necessary to consider only one of them in detail, say temperature, when effecting the correlation. Here it is seen that prior to about 340 years ago both $G_{ma}(t)$ plot and the temperature (and hence inversely raininess and cloudiness) exhibit an approximately 272 year periodicity whereas later than that an approximately 136 year periodicity is evident in both. This may reflect the increased accuracy of data recording over the more recent period rather than a real physical feature. It should be noted that it is unfortunate that the moving average technique applied to the original G(t) data to derive the smoothed $G_{ma}(t)$ plot has disguised the trough known to be present in the original data at the point marked by the hollow arrow about 130 years ago.

Japan

Only one Japanese climate-related variable is compared on Figure 8 with the $G_{ma}(t)$ plot over the same relatively recent period of 600 years as already investigated in relation to Chinese climate. This is the variation of the freezing date of Lake Suwa portrayed by Lamb (1977). Major arrows indicating maxima and minima have been inserted at exactly the same points on the $G_{ma}(t)$ plot as on Figure 7. Here it is seen that these maxima and minima are reflected by the general variation of the freezing date. The hotter the climate predicted from the $G_{ma}(t)$ plot, the earlier is the freezing date, representing an inverse relation between Japanese and global temperature variation on this timescale. This emphasises the non-synchronous timing of the little ice age throughout the world observed by many workers and the inverse relation also demon-

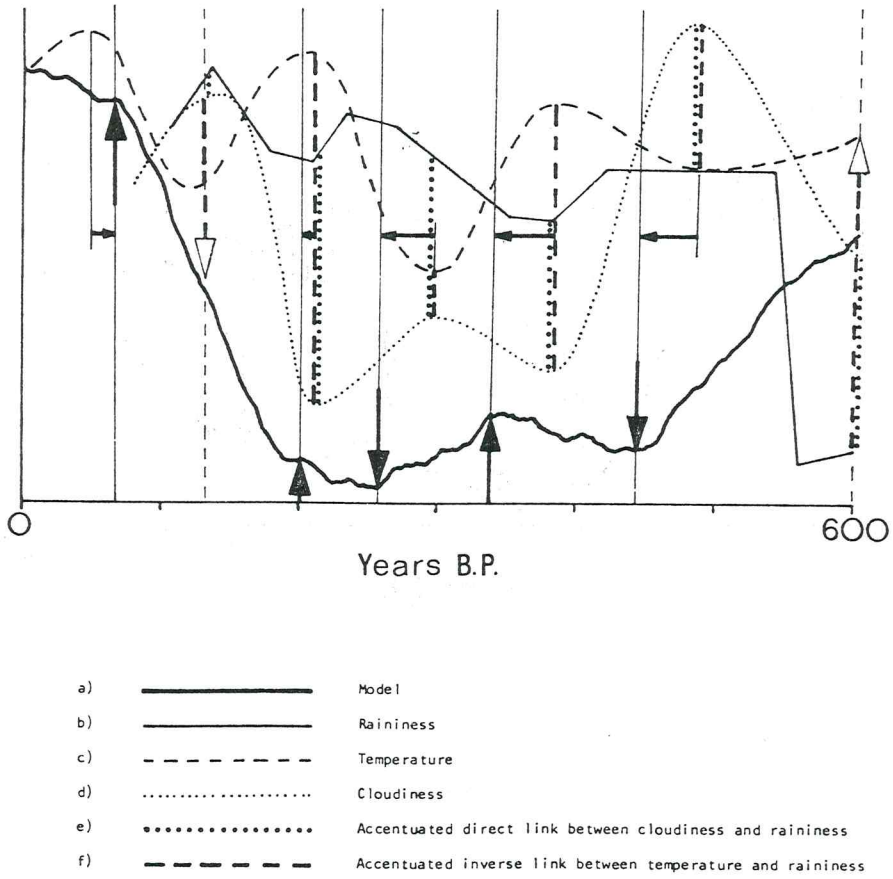

Figure 7 Comparison of Chinese climatic indices and model over most recent 600 years

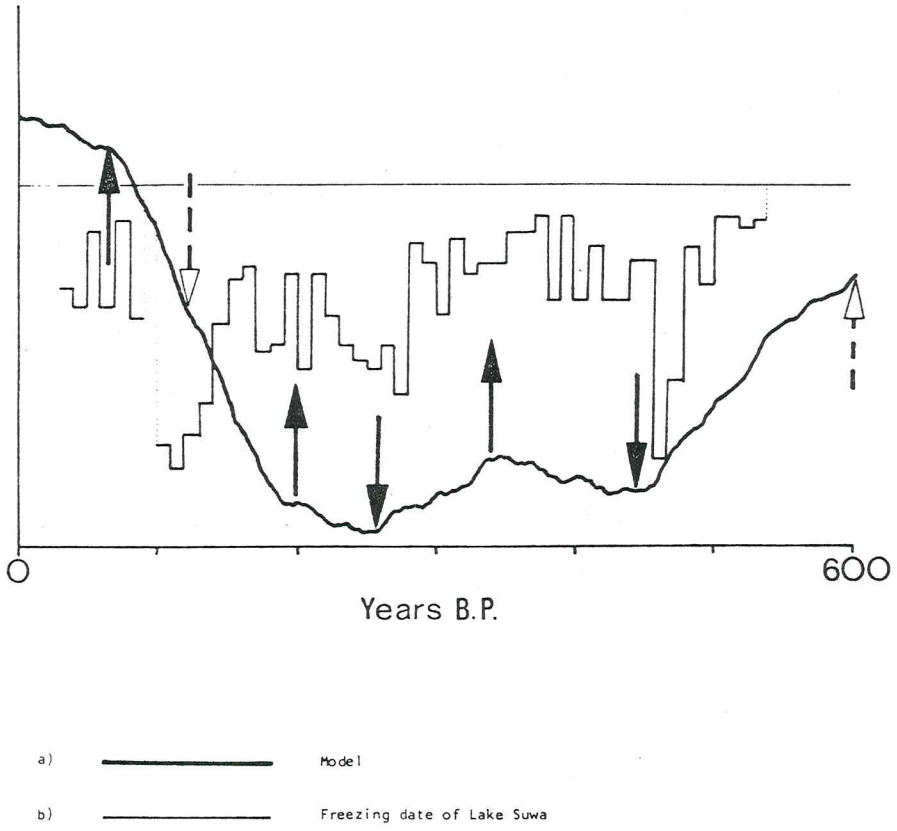

Figure 8 Comparison of Japanese climatic index and model over most recent 600 years

strated by the global climate modelling of Wigley *et al.* (1980).

Applying the climate model

Now that the model has been shown to be as applicable to East Asia (once calibrated as shown in the previous section) as to the parts of the world from which it was derived, it is appropriate to consider how it might be applied to matching in hindcast certain climate-related variables which are of great significance to a part of East Asia. Success in that endeavour would open the way to forecasting the return period of enhanced occurrence because the model has a predictive as well as hindcasting capability. Let us consider the problem of landslipping.

Landslips have bedevilled Hong Kong for many years, ever since the crowded conditions of the coastal area forced development on the neighbouring unstable slopes. Unfortunately a longterm record of landslip activity in Hong Kong has not been available to the writer. Nevertheless, provided it is possible to correlate landslip activity with the $G_{ma}(t)$ plot of the climatic model for any other area, sufficient has been shown here in establishing East Asian calibrations to indicate that an equivalent correlation should be forthcoming for Hong Kong.

Turning to Figure 9, it is seen that such a correlation does indeed exist, albeit for western Norway. The major arrows indicating general maxima with included minimum on the $G_{ma}(t)$ curve indicate respectively times of generally negligible and intense landslipping over the past 400 years. The landslip data (representing numbers of landslip events in a fixed period) have been prepared from histograms presented by Grove (1972) as has the corresponding information about floods: it should be noted that the coincidence of floods and landslips is very marked. The intermediate arrows indicate maxima and minima on the $G_{ma}(t)$ plot while the minor arrows represent extensions of these indicators to the flood and landslip variation curves. It is seen that the majority of maxima and minima even in the short term correlate closely between the climatic model and the observed data. This is to be expected from further reference to the global climate mapping of Wigley *et al.* (1980) which indicates that the most southerly third of Norway and that containing about 90 per cent of its population becomes drier with increasing global temperature. The flood and landslip record will reflect the number of observers (a geographical factor) as much as the temporal variation so that in this case "western Norwegian landslips and floods" really implies mainly those landslips and floods in the most southerly third of western Norway. This clearly explains the correlations.

In turn Figure 10 provides an English example of the rate of retreat of the head of an individual coastal landslip during most of the twentieth century, again correlated with the $G_{ma}(t)$ plot. These data are taken from Denness *et al.* (1975) who were unfortunately able, with the aid of historical Ordnance Survey maps and resurveying, to determine the

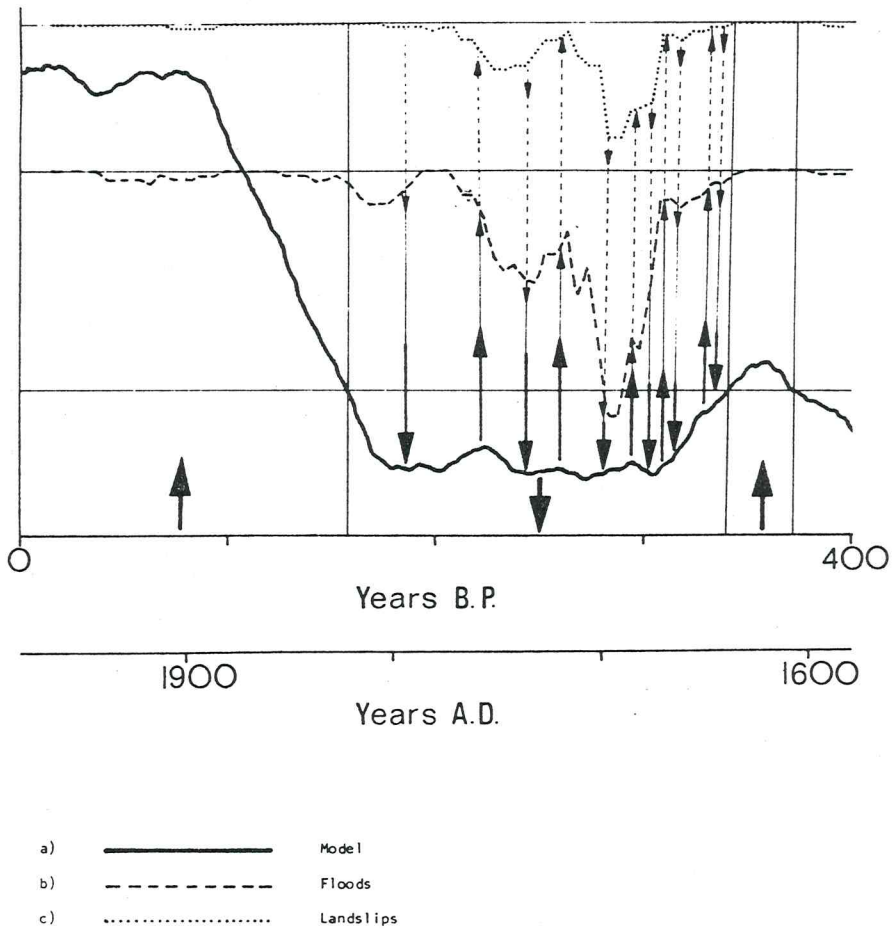

Figure 9 Comparison of incidence of landslips and floods with model over most recent 400 years

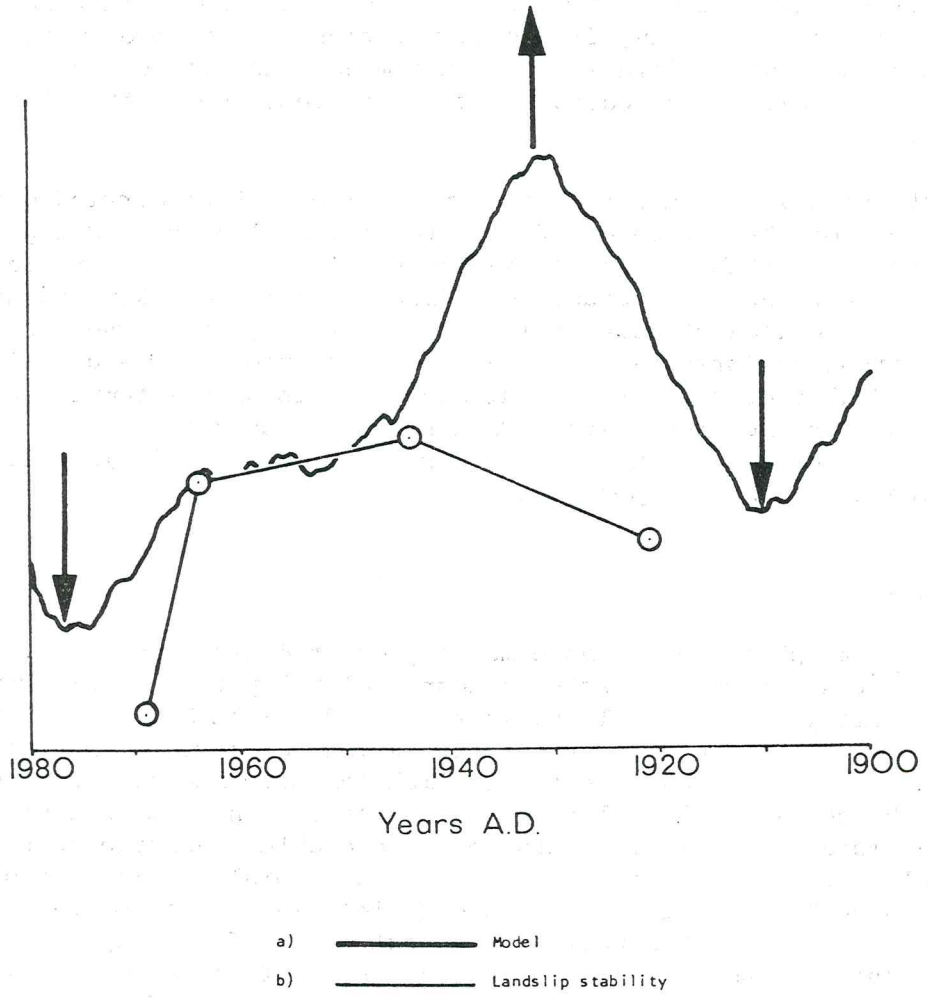

Figure 10 Comparison of individual landslip stability with model during twentieth century A.D.

position of the landslip head on only five occasions giving the four relative local landslip stability (the inverse of the rate of retreat) points on the diagram. Nevertheless it is seen that the general trend of the $G_{ma}(t)$ plot with the two minima separated by a maximum is approximated by the local landslip stability variation; the rate of retreat was less during the middle years of this century at a time when the global temperature was generally hotter. Wigley *et al.* (1980) again provide the link — as global temperature rises England becomes drier. As Denness *et al.* point out the landslip is significantly influenced by groundwater which in turn results, albeit partially indirectly, from precipitation. Therefore, with increased temperature and lower rainfall during the middle decades of this century the landslip stability increased naturally in response to the climatic variation.

In the Hong Kong context, Malone and Shelton (1982) carried out a short-term analysis of the influence of climate on landslipping. Using data collected after the establishment of systematic landslip recording in Hong Kong in 1978 they were able to deduce that "landslips in Hong Kong occur during or soon after periods of heavy rainfall". This is, of course, consistent with the foregoing Norwegian and English observations. The global climatic mapping of Wigley *et al.* (1980) indicates that as global temperature increases Hong Kong becomes drier. Therefore, in concert the work of Wigley *et al.* and Malone and Shelton points towards a decrease in landslip activity with increasing global temperature.

Discussion

The $G_{ma}(t)$ plot, the climate model presented here, models global temperature. It has been successfully tested globally to a sensitivity of periodic variations down to 1,090 years, and for East Asia to a sensitivity of 136 years; there are also strong suggestions of correlatable periodicities down to about 68 years in the English landslip record and about 17 years in the Norwegian landslip and flood data. Hence it is logical to pursue the model into higher frequencies to enable advantage to be taken, for example, of the association of decreased rainfall in Hong Kong with increased global temperature and the parallel association of rainfall with landslips. This will form part of the next phase of development of the model and should lead to a soundly based general forecasting model of, among many other environmental hazards of economic significance, Hong Kong landslipping.

Conclusions

In summary, it is suggested that the evidence examined here is supportive of the reinforcement of the climatic model previously developed, thereby extending its application range from billions of years to the historical timescale. East Asian examples are as consistent with the model as are those from other sites throughout the world. Extension of the model to

higher frequency global temperature variation permits successful hindcasting of landslip activity and flooding in Norway with consequent implications, among many others, for potential landslip forecasting in Hong Kong.

References

BLOOM, A.L. (1971) Glacio-eustatic and isostatic controls of sea level since the last glaciation. pp. 355-380 in *The Late Cenozoic Glacial Ages* (ed. K.K. Turekian). Yale University Press, New Haven.

BRAY, J.R. (1968) Glaciation and solar activity since the fifth century B.C. and the solar cycle. *Nature* 220:640-642.

CHU Ko-Chen (1973) A preliminary study on the climatic fluctuations during the last 5000 years in China. *Scientia Sinica* 16:226-256.

CHURCHILL, D.M. (1968) The distribution and prehistory of *Eucalyptus Diversicolour, E.marginata* and *E.calophylla* in relation to rainfall. *Australian J. Bot.* 16:125-151.

DANSGAARD, W., JOHNSEN, S.J., CLAUSEN, H.B. and LANWAY, C.C. (1971): Climatic record revealed by the Camp Century ice core. pp. 37-56 in *The Late Cenozoic Glacial Ages* (ed. K.K. Turekian). Yale Univ. Press, New Haven.

DENNESS, B. (1981) How to build an ocean. pp. 341-344 in *Proc. Conf. Oceans 81,* IEEE, Boston.

DENNESS, B. An analytical climate model: application to the southern hemisphere Quaternary period. *Proc. Int. Symp. on Late Cainozoic Palaeoclimates of the Southern Hemisphere.* SASQUA, Pretoria, South Africa. (in press).

DENNESS, B., CONWAY, B.W., McCANN, D.M. and GRAINGER, P. (1975) Investigation of a coastal landslip at Charmouth, Dorset. *Q.Jl. Engng.Geol.* 8:119-140.

GROVE, J.M. (1972) The incidence of landslides, avalanches and floods in western Norway during the Little Ice Age. *Arctic and Alpine Res.* 4(2):131-138.

HAMMEN, Van der, T., MAARLEVELD, G.C., VOGEL, J.C. and ZAGWIJN, W.H. (1967). Stratigraphy, climatic succession and radiocarbon dating of the last glacial in the Netherlands. *Geologie en Mijnbouw* 46:79-95.

HAMMEN, Van der, T., WIJMSTRA, T.A. and ZAGWIJN, W.H. (1971) The floral record of the Late Cenozoic of Europe. pp. 391-424 in *The Late Cenozoic*

Glacial Ages (ed. K.K. Turekian). Yale Univ. Press, New Haven.

HAYS, J.D., SAITO, T., OPDYKE, N.D. and BURCKLE, L.H. (1969) Pliocene-Pleistocene sediments of the equatorial Pacific: their paleomagnetic, biostratigraphic and climatic record. *Geol.Soc. Am. Bull.* 80:1481-1513.

HEUSSER, C.J. (1966) Polar hemispheric correlation: palynological evidence from Chile and the Pacific north-west of America. pp. 124-141 in *World Climate 8000-0 B.C.* (ed. J.S. Sawyer). Roy. Met. Soc., London.

IMBRIE, J. and KIPP, N.G. (1971) A new micropalaeontological method for quantitative palaeoclimatology: application to a Late Pleistocene Caribbean core. pp. 71-181 in *The Late Cenozoic Glacial Ages* (ed. K.K. Turekian). Yale Univ. Press, New Haven.

LA MARCHE, V.C. (1973) Holocene climatic variations inferred from tree-line fluctuations in the White Mountains, California. *Quaternary Res.* 3:632-660.

LA MARCHE, V.C. (1974) Palaeoclimatic inferences from long tree-ring records, *Science* 183:1043-1048.

LAMB, H.H. (1977) *Climate: present, past, and future, 2, Climatic history and the future.* Methuen, London. 835 pp.

LINK, F. (1958) Kometen, Sonnentätigkeit und Klimaschwankungen. *Die Sterne* 34:129-140.

MALONE, A.W. and SHELTON, J.C. (1982) Landslides in Hong Kong 1978-1980. *Jl. Geot. Eng. Div., ASCE,* 108:425-442.

MARKGRAF, V. (1974) Palaeoclimatic evidence derived from timberline fluctuations. pp. 67-83 in *Les Méthodes quantitatives d'étude des variations du climat au cours du Pléistocène* (ed. J. Labeyrie). Colloques internat. du C.N.R.S. No. 219, C.N.R.S. Paris.

SCHOVE, D.J. (1949) Chinese "Raininess" through the centuries. *Met. Mag.* 78:11-16.

SHACKLETON, N.J. and KENNETT, J.P. (1975) Late Cenozoic oxygen and carbon isotope changes at DSDP Site 284. pp. 801-807 in *Initial reports of the Deep Sea Drilling Project.* 29, U.S. Government Printing Office, Washington, D.C.

VAN DONK, J. (1976) 18_0 record of the Atlantic Ocean for the entire Pleistocene Epoch. pp. 147-163 in *Investigation of Late Quaternary Palaeo-oceanography* (eds. R.M. Cline and J.D. Hays). Geol. Soc. Am.Mem. 145.

WEST, P.G. (1972) *Pleistocene geology and biology*. Longman, London, 202-206.

WIGLEY, T.M.L., JONES, P.D. and KELLY, P.M. (1980) Scenario for a warm, high CO_2 world. *Nature* 283:17-21.

YAO Shan-Yu (1943) The geographical distribution of floods and droughts in Chinese history 206BC-AD1911. *Far East Quarterly*, 357.

YAO Shan-Yu (1944) Flood and drought data in the T'u-shu Chi Chung and Ch'ing Shi Cao, *Harvard J. Asiatic Studies* 8:214.